Novel Bruch's Membrane Opening Minimum Rim Area Equalizes Disc Size Dependency and Offers High Diagnostic Power for Glaucoma

Philip Enders,[1] Werner Adler,[2] Friederike Schaub,[1] Manuel M. Hermann,[1] Thomas Dietlein,[1] Claus Cursiefen,[1] and Ludwig M. Heindl[1]

[1]Department of Ophthalmology, University Hospital of Cologne, Cologne, Germany
[2]Department of Medical Informatics, Biometry, and Epidemiology, Friedrich-Alexander University Erlangen-Nuremberg, Erlangen, Germany

Correspondence: Philip Enders, Department of Ophthalmology, University of Cologne, Kerpener Strasse 62, 50924 Cologne, Germany; philip.enders@uk-koeln.de.

Submitted: August 19, 2016
Accepted: October 30, 2016

Citation: Enders P, Adler W, Schaub F, et al. Novel Bruch's membrane opening minimum rim area equalizes disc size dependency and offers high diagnostic power for glaucoma. *Invest Ophthalmol Vis Sci*. 2016;57:6596–6603. DOI:10.1167/iovs.16-20561

Purpose. The purpose of this study was to assess the diagnostic power of the novel two-dimensional parameter Bruch's membrane opening minimal rim area (BMO-MRA) in spectral-domain optical coherence tomography (SD-OCT) for detection of glaucoma compared to minimal rim width (BMO-MRW) and retinal nerve fiber layer (RNFL) thickness in large and small optic discs.

Methods. In this case-control, cross-sectional study, 207 eyes of 207 participants, including 89 controls and 97 patients with glaucoma and 21 with ocular hypertension (OHT), with a disc size <1.63 mm^2 or >2.43 mm^2 underwent SD-OCT, confocal laser scanning tomography (CSLT), visual field testing, and clinical examination. Bruch's membrane opening-MRA BMO-MRW, RNFL thickness of SD-OCT and disc margin rim area (DM-RA) of CSLT were evaluated and analyzed for diagnostic power to detect glaucoma.

Results. In healthy eyes with macrodiscs, mean BMO-MRW of 243.14 ± 43.12 μm was significantly smaller than BMO-MRW in microdiscs (338.97 ± 69.39; $P < 0.001$). Bruch's membrane opening-MRA was comparable between disc size groups with 1.22 ± 0.25 mm^2 for macrodiscs and 1.26 ± 0.27 mm^2 for microdiscs ($P = 0.51$), as was RNFL thickness (82.69 ± 15.76 μm versus 78.53 ± 11.01 μm, respectively; $P = 0.28$). Perimetric mean deviation was −8.7 ± 6.3 dB in glaucoma and −0.6 ± 1.60 dB in OHT patients. Correlation of BMO-MRA and visual field function was rho (ρ) = 0.70 ($P < 0.001$). Diagnostic power to differentiate glaucoma patients was highest for BMO-MRA. Partial area under the curve (pAUC) for BMO-MRA was 0.14 for specificity between 0.8 and 1.0, exceeding pAUCs of BMO-MRW ($P < 0.001$), RNFL thickness ($P = 0.03$), and DM-RA ($P = 0.01$).

Conclusions. Bruch's membrane opening-based minimum rim area measurements offer advantages compared to one-dimensional parameters assessing neuroretinal rim by SD-OCT. In nonglaucomatous eyes, BMO-MRA values seem comparable for the full range of disc sizes. Bruch's membrane opening-MRA surpasses other parameters in diagnostic power for glaucoma.

Keywords: Bruch's membrane opening, glaucoma detection, minimum rim area, morphometry, novel OCT parameter

Bruch's membrane opening (BMO)-based spectral-domain optical coherence tomography (SD-OCT) has been introduced for diagnosis and follow-up of glaucoma. The technique seems to surpass the previous clinical standard of morphometric optic nerve head (ONH) analysis, confocal scanning laser tomography (CSLT) measurement, diagnostic power, and observer independence.[1–3] Spectral-domain OCT assesses the ONH and retinal structures between Bruch's membrane opening (BMO) and the internal limiting membrane (ILM). Additionally, subsurface structures are analyzed.[4]

Optical coherence tomography (Spectralis, Heidelberg Engineering, Heidelberg, Germany) evaluation software was used to calculate BMO-based minimum rim width (BMO-MRW) and peripapillary retinal nerve fiber layer (RNFL) both globally and localized for optic disc sectors.[1,4–11] Other one-dimensional rim based parameters, such as horizontal rim width (BMO-HRW) and perpendicular rim width (BMO-PRW) have also been evaluated. Morphometric ONH parameters' correlation with visual field function has been analyzed in numerous studies.[1,12–20]

Despite major advantages in glaucoma diagnostics compared to preceding techniques, BMO-based morphometry using one-dimensional parameters (i.e., BMO-MRW) has important limitations. Normative BMO-MRW values depend on disc size, especially in large optic discs BMO-MRW is physiologically thinner. Recently, morphometric data for eyes with non-glaucomatous macrodiscs have been published.[19] Other less frequent ONH configurations (e.g., conus, myopic disc) require matching with a specific control group of healthy individuals to achieve high diagnostic power. Malik et al.[21] published an

analysis of the diagnostic power in myopic discs; Enders et al.[22] assessed the diagnostic power of one-dimensional SD-OCT-based morphometric parameters in microdiscs independently of refractive status.

As an advancement of the technique, Gardiner et al.[1] introduced the two-dimensional parameter BMO-based minimum rim area (BMO-MRA), analyzing 221 eyes. Those authors concluded that MRA measurements using SD-OCT are significantly better correlated to both RNFL thickness and mean deviation in visual field testing than rim measurements within the BMO plane or based on the clinical disc margin. Additionally, BMO-MRA is supposed to equalize rim width differences between very small ONHs and very large ONHs. In calculating BMO-MRA, disc size serves as an input parameter and should compensate for differences in minimum neuroretinal rim width related to disc size.

The present study's purpose was to assess the diagnostic power of BMO-based MRA measurements in individuals with very small and very large ONHs, referred to as microdiscs (<1.63 mm^2 in CSLT) and macrodiscs (> 2.43 mm^2 in CSLT), respectively. Bruch's membrane opening-MRA was calculated by a newly developed OCT evaluation software. We aimed to verify the hypothesis that the novel parameter BMO-MRA neutralizes the effect of disc size on one-dimensional morphometric parameters. We also aimed to assess the diagnostic power of BMO-MRA to differentiate healthy small/large ONHs from those with glaucomatous damage compared to BMO-MRW, RNFL thickness (OCT), and rim area (CSLT). The study cohort consisted of nonglaucomatous individuals and glaucomatous patients examined at the center.

Methods

Data for this single-center retrospective analysis were acquired between September 2014 and February 2016 at the Department of Ophthalmology, University Hospital of Cologne, Germany. Patients in whom both CSLT and SD-OCT measurements of the optic nerve head were made on the same day were screened for disc size. Additional parameters were collected from patients' files, including ophthalmologic diagnoses, previous surgery (especially if antiglaucomatous), best-corrected visual acuity, IOP at examination and maximal IOP, topical medication, and medical history of the eyes. Intraocular pressure was assessed by corneal rebound tonometry (TA01i tonometer, Icare Finland Oy, Vantaa, Finland) in adults and children, respectively, and by Goldmann tonometry. All patients included in this study were patients examined at our center. Individuals with no suspicion of glaucoma underwent ONH morphometry and visual field testing as part of a full screening for ocular diseases or for exclusion of glaucoma or ocular hypertension (OHT), mainly on a private medical practice basis.

Inclusion and Exclusion Criteria

Eyes with small optic discs of less than 1.63 mm^2 in CSLT, as well as those with a large optic disc of more than 2.43 mm^2 in CSLT, were included in this study. This threshold was set by exceeding the lower or upper limit for the normative collective in CSLT according to CSLT software version 3.1.0.2. The exclusion criteria were visual field loss for causes other than glaucoma; unsatisfactory image quality in CSLT, OCT, or in visual field testing; and best-corrected visual acuity >0.4 logMAR (Snellen equivalent: 20/50). The interval of SD-OCT/CSLT assessment and visual field testing should not have exceeded ± 28 days. For nonglaucomatous individuals, a mean deviation of better than −3 dB was required. If multiple data points at different time points were available, the examination with the best imaging quality indicators was used. If both eyes fulfilled all inclusion criteria and no exclusion criteria, the eye with the smaller or respectively larger disc size was selected.

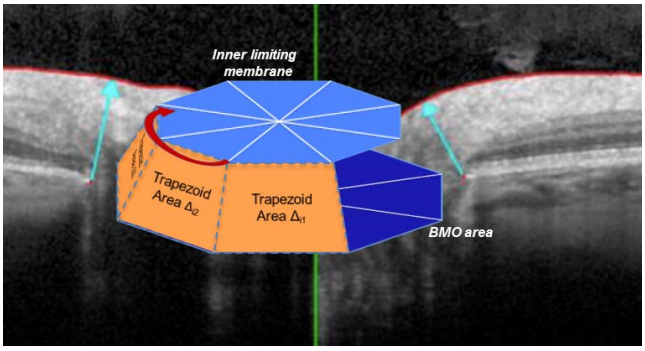

Figure 1. Principle of standardized BMO-MRA calculation software Spectralis SP-X VWM. Note in the graphical model: between every two B-scans, local BMO-based minimum rim area is calculated as a trapezoid covering the minimum area between the ILM and BMO. Global and sectorial BMO-MRA are determined by addition of respective local minimum rim area results.

Diagnosis of Glaucoma

Patients were divided into one of three diagnostic groups according to the Guidelines of the European Glaucoma Society (EGS)[23]: glaucoma patients, patients with OHT, and individuals with no suspicion of glaucoma.

In EGS guidelines, glaucomas are progressive optic neuropathies which have common characteristic morphologic changes at the ONH and RNFL in the absence of other ocular diseases or congenital anomalies. Progressive ganglion cell death and visual field loss are associated with these changes. For glaucoma patients included in the present study, beginning changes in visual field assessment were required. Perimetric data were reviewed manually for glaucomatous changes according to EGS guidelines.[23] Perimetric data were reviewed manually for glaucomatous changes according to EGS guidelines. Comprehensive grading and screening for glaucomatous defects in visual field consisted of evaluation of mean deviation, mean pattern standard deviation, grayscale map, Bebié curve, and pattern deviation probability maps.

Morphometric Analyses of the Optic Disc

CSLT and SD-OCT examinations were performed (Heidelberg Engineering Retina Tomograph III and Spectralis-SD-OCT; Heidelberg Engineering) in accordance with standard operating procedures. Two independent evaluators (EP, SF) assessed image quality and, in CSLT, defined the disc margin manually; the threshold for the standard deviation of the CSLT topography was set at <40 µm. Data included in OCT consisted of an image quality index of >15 dB. The neuroretinal rim was calculated automatically by using the CSLT standard reference plane. Spectral-domain OCT imaging was performed with a commercially available OCT device. A light source of 870 nm was used according to standard imaging procedure. The scanning pattern was centered on the BMO with radial equidistance (24-high resolution, 15° radial scans, each averaged from 27 B-scans). The examiners controlled the centration of the scan to the optic disc and corrected errors in detection of ILM and BMO. Optical coherence tomography-based parameters were calculated using the device-operating software tool provided by the manufacturer, including provision of a data export batch.

Table 1. Epidemiologic and Baseline Data

Parameter	Nonglaucomatous Subjects, $n = 89$	Glaucomatous Subjects, $n = 97$	Ocular Hypertension, $n = 21$
Sex (%)			
Number of men	41 (46.1)	40 (41.2)	12 (57.1)
Number of women	48 (53.9)	57 (58.8)	9 (42.9)
Age, y			
Mean ± SD	41.7 ± 24.6	68.5 ± 11.6	56.3 ± 11.9
Median	43.0	72.0	57.0
Range	4–86	22–88	34–79
Number of eyes (%)			
Right	40 (44.9)	47 (48.5)	10 (47.6)
Left	49 (55.1)	50 (51.5)	11 (52.4)
BCVA logMAR (Snellen equivalent)			
Mean ± SD	0.03 ± 0.09 (20/20)	0.17 ± 0.19 (20/32)	0.05 ± 0.11 (20/25)
Median	0 (20/20)	0.1 (20/25)	0 (20/20)
Spherical equivalent, D			
Mean ± SD	−0.72 ± 2.23	−0.66 ± 2.25	−1.43 ± 3.68
Median	−0.08	0	0
IOP, mm Hg			
Mean ± SD	16.9 ± 3.8	17.9 ± 7.3	18.2 ± 5.2
Median	18.0	16.0	18.0
Mean deviation (dB) of 30/2 visual field testing			
Mean ± SD	−0.6 ± 1.60	−8.7 ± 6.3	−0.8 ± 1.2
Median	−0.8	−7.5	−0.7
Types of glaucoma (%)	NA		NA
Primary open angle		78 (80.4)	
Pseudoexfoliation		13 (13.4)	
Pigmentary		2 (2.1)	
Chronic closed angle		4 (4.1)	

BCVA, best-corrected visual acuity; dB, decibel; IOP, intraocular pressure; NA, not applicable.

Bruch's membrane opening-MRA calculation was performed by the manufacturer's software, Spectralis SP-X VWM (Heidelberg Engineering), provided without charge. Gardiner et al.[1] proposed the principle of BMO-MRA calculation. Bruch's membrane opening-MRA is described as the minimum surface spanned between BMO and ILM (Fig. 1). The minimum surface tends to be approximately perpendicular to the direction of nerve fibers traversing the ONH. Thus, the minimum surface tends to correlate with the total number of nerve fibers traversing the optic nerve. In BMO-MRA, the analog to procedures in one-dimensional morphometric parameter MRW, the calculation software used localized minimization of every radial scan independently of other sectors.

Visual Field Testing

Visual field testing was performed using a visual field analyzer (Octopus 101, Haag-Streit AG, Koeniz, Switzerland) with a 30-2 tendency-oriented perimetry white-on-white standard pattern. Data analysis was performed using Peridata version 3.1 software (PeriData Software GmbH, Huerth, Germany). Visual field testing was performed separately for both eyes; lens correction matching age and refraction were applied. Thresholds for reliability were set at ≤30% for false positive and false negative answers and at ≤20% for fixation losses. Mean deviation (MD) was analyzed for all patients. Visual field results were screened manually as described above for

Table 2. Morphometric Parameters in Nonglaucomatous Controls in Relation to Disc Size

Parameter	Macrodiscs		Microdiscs		*P* Value	Differences of Means	95% CI for Differences of Means
	Mean	95% CI	Mean	95% CI			
BMO-MRW, µm	243.14	232.86–253.42	338.97	305.53–372.42	<0.001	95.84	61.13 to 130.54
RNFLT, µm (SD-OCT)	82.69	78.93–86.44	78.64	73.19–83.87	0.28	−4.16	−11.83 to 3.51
BMO-MRA, mm²	1.22	1.16–1.28	1.26	1.14–1.39	0.52	0.04	−0.09 to 0.17
Rim area, mm² (CSLT)	1.54	1.46–1.62	1.05	0.97–1.13	<0.001	−0.48	−0.59 to −0.37

BMO-MRW, Bruch's membrane opening minimal rim width; CI, confidence interval; CSLT, confocal scanning laser tomography; ONH, optic nerve head; RNFLT, retinal nerve fiber layer thickness; SD-OCT, spectral-domain optical coherence tomography.

glaucomatous scotoma and were classified using the method reported by Aulhorn.[24–26]

Sample Size

The sample size required to detect a clinically relevant improvement of 0.2 in an assumed area under curve (AUC) of 0.7 with power 0.8 and type I error alpha set to 0.05 was estimated to be at least 52 patients in each group.[27]

Ethics and Statistics

According to national medical regulations for retrospective single-center clinical studies, Ethics Committee of the University of Cologne ruled that approval was not required for this study. All tenets of the Declaration of Helsinki were observed. Statistical analyses were performed using SPSS version 22.0 software (SPSS, IBM Corp. Armonk, NY, USA) and the statistical programming language R version 3.2.2 (R Foundation for Statistical Computing, Vienna, Austria). Pearson's correlation coefficient r value and Spearman rank correlation coefficient rho (ρ) were used depending on normal distribution of parameters. Student's t-test or the Kolmogorov-Smirnov Z test was applied for comparing means depending on normal distribution tested by the Shapiro-Wilk test. Diagnostic power was assessed by the receiver operating characteristic (ROC) analysis and tested for statistically significant differences with the DeLong test for areas under curve. P values for partial areas under curve were estimated by bootstrap. The threshold for statistical significance was set to a P value of <0.05.

Results

A total of 207 eyes of 207 patients were included in this study. Glaucoma was diagnosed in 97 patients (46.9%); OHT was present in 21 patients (10.1%), and 89 individuals (43.0%) showed no clinical suspicion of glaucoma. Epidemiology and baseline data are summarized in Table 1.

Nonglaucomatous Controls

Mean disc size (CSLT) in 70 eyes with macrodiscs was 2.98 ± 0.41 mm² (range, 2.45–4.23 mm²) and 1.34 ± 0.22 mm² (range, 0.91–1.60 mm²) in 19 microdiscs. The corresponding mean BMO area was 2.49 ± 0.42 mm² (range, 1.72–3.35 mm²) and 1.59 ± 0.22 mm² (range, 1.23–2.12 mm²), respectively. Mean BMO-MRW ($P < 0.001$) was significantly lower in eyes with large ONHs than in eyes with microdiscs, whereas DM-RA was significantly higher in macrodiscs ($P < 0.001$). In contrast, mean BMO-MRA ($P = 0.51$) and peripapillary RNFL ($P = 0.28$) were comparable between both of the disc size groups (Table 2). Table 3 displays global morphometric parameter including sectorial data.

Glaucoma Patients

In 97 glaucomatous eyes, mean best-corrected visual acuity was 0.17 ± 0.19 logMAR (20/32); mean deviation of 30-2 visual field testing was –8.5 ± 6.43 dB.

Mean disc size (CSLT) in 44 eyes with macrodiscs was 2.80 ± 0.28 mm² (range, 2.44–3.72 mm²) and 1.39 ± 0.19 mm² (range, 0.90–1.62 mm²) in 53 microdiscs. Corresponding mean BMO area was 2.41 ± 0.34 mm² (range, 1.93–3.42 mm²) and 1.36 ± 0.35 mm² (range, 0.93–2.36 mm²), respectively. Table 3 displays global morphometric parameter including sectorial data. Pearson correlation coefficients between BMO-based parameters MRW and MRA ranged from

Table 3. Global and Sectorial Morphometric Parameters in ONH Analysis

Global Parameter	Sectorial Parameter	Gobal	Nasal	Nasal Superior	Nasal Inferior	Temporal	Temporal Superior	Temporal Inferior
Normal controls	BMO-MRA, mm² ± SD	1.21 ± 0.3	0.38 ± 0.1	0.15 ± 0.0	0.17 ± 0.0	0.24 ± 0.1	0.13 ± 0.0	0.16 ± 0.0
	BMO-MRW, µm	263.60 ± 63.3	277.10 ± 77.8	285.15 ± 89.0	326.58 ± 81.8	201.70 ± 49.4	251.15 ± 72.6	293.70 ± 64.8
	RNFLT, µm (SD-OCT)	81.80 ± 15.0	62.79 ± 14.7	112.52 ± 24.4	125.82 ± 23.3	65.93 ± 16.7	90.34 ± 28.1	86.09 ± 25.3
	DM-RA, mm² (CSLT)	1.43 ± 0.4	0.43 ± 0.1	0.21 ± 0.1	0.22 ± 0.1	0.22 ± 0.1	0.17 ± 0.1	0.19 ± 0.1
Glaucoma	BMO-MRA, mm²	0.77 ± 0.3	0.25 ± 0.1	0.09 ± 0.0	0.10 ± 0.0	0.15 ± 0.1	0.07 ± 0.0	0.08 ± 0.0
	BMO-MRW, µm	178.86 ± 85.6	201.83 ± 108.0	200.80 ± 101.7	214.6 ± 113.2	140.61 ± 61.6	153.27 ± 91.1	170.15 ± 101.7
	RNFLT, µm (SD-OCT)	58.23 ± 16.1	46.16 ± 17.0	62.32 ± 23.6	59.78 ± 23.2	54.32 ± 17.4	74.93 ± 29.2	78.05 ± 36.4
	DM-RA, mm² (CSLT)	0.87 ± 0.3	0.27 ± 0.1	0.14 ± 0.1	0.14 ± 0.1	0.14 ± 0.1	0.09 ± 0.1	0.10 ± 0.1
Ocular hypertension	BMO-MRA, mm²	1.17 ± 0.3	0.36 ± 0.1	0.13 ± 0.0	0.15 ± 0.0	0.21 ± 0.0	0.11 ± 0.0	0.14 ± 0.0
	BMO-MRW, µm	262.64 ± 72.8	285.45 ± 92.9	277.37 ± 98.6	335.93 ± 99.4	195.6 ± 48.1	239.19 ± 69.8	286.60 ± 76.8
	RNFLT, µm (SD-OCT)	74.05 ± 15.6	56.71 ± 18.3	82.52 ± 28.2	82.52 ± 28.2	59.81 ± 10.7	105.05 ± 21.8	114.52 ± 28.8
	DM-RA, mm² (CSLT)	1.38 ± 0.5	0.38 ± 0.0	0.20 ± 0.0	0.21 ± 0.1	0.23 ± 0.1	0.17 ± 0.1	0.19 ± 0.1

BMO-MRW, Bruch's membrane opening minimal rim width; CSLT, confocal scanning laser tomography; DM-RA, disc margin rim area; ONH, optic nerve head; RNFLT, retinal nerve fiber layer thickness; SD-OCT, spectral-domain optical coherence tomography.

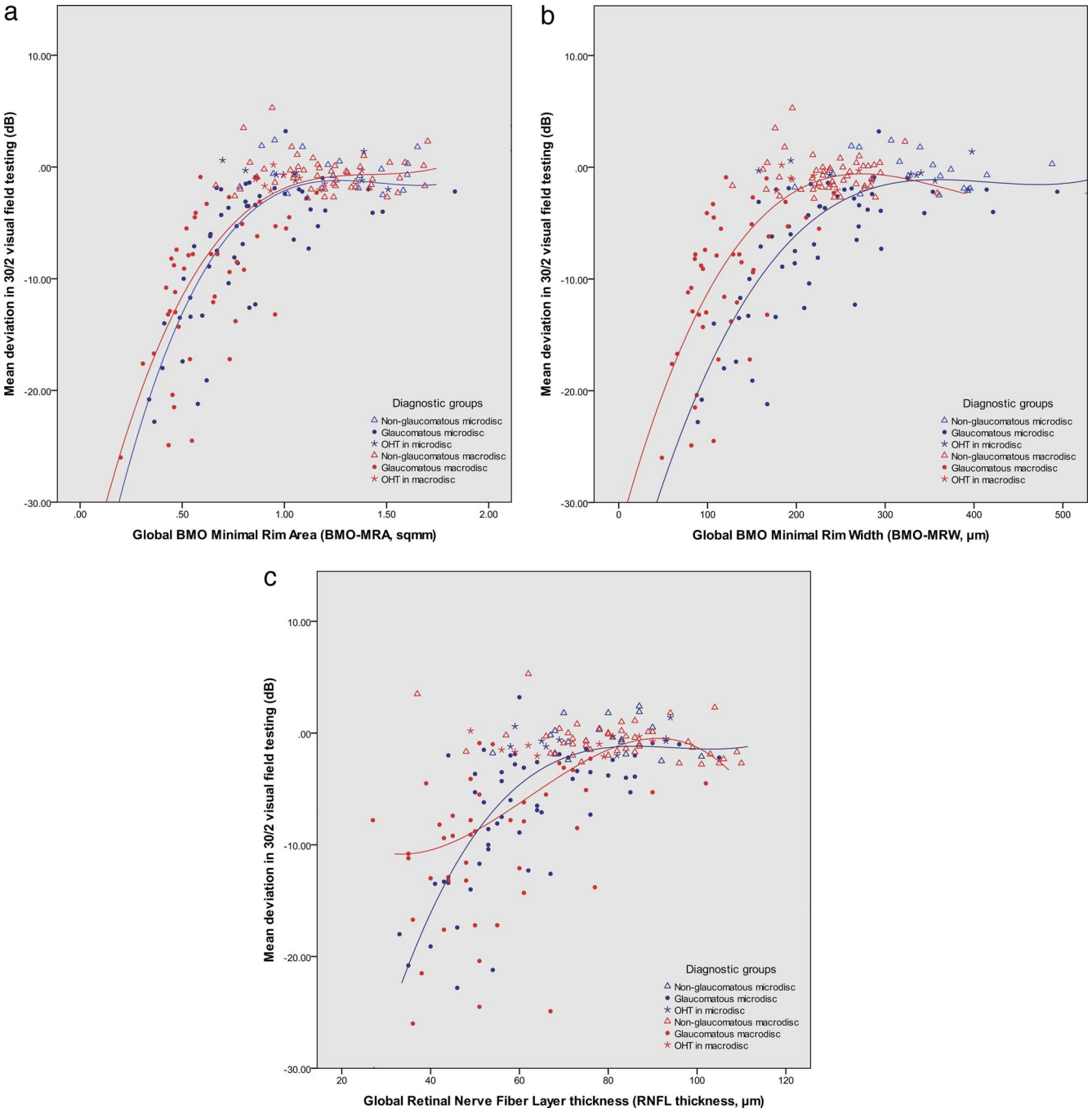

Figure 2. (**a**) Scatter plot of BMO-MRA and mean deviation of visual field function in macro- and microdiscs Note, fitted curves are based on a cubic curve estimation regression model. (**b**) Scatter plot of BMO-MRW and mean deviation of visual field function in macro- and microdiscs. Note, fitted curves are based on a cubic curve estimation regression model. (**c**) Scatter plot of RNFL thickness and mean deviation of visual field function in macro- and microdiscs. Note, fitted curves are based on cubic curve estimation regression model.

0.92 to 0.99 ($P < 0.001$); correlations between peripapillary RNFL thickness to BMO-based parameters were between an r of 0.72 and 0.76 ($P < 0.001$). Correlation between RNFL and disc margin rim area (DM-RA) was 0.43 ($P < 0.001$). The visual field mean deviation demonstrated a significant correlation with BMO-MRA ($\rho = 0.70$; $P < 0.001$). Correlation between BMO-MRW and mean deviation ($\rho = 0.67$; $P < 0.001$) was comparable ($P = 0.39$), whereas correlations of RNFL thickness and mean deviation ($\rho = 0.58$; $P < 0.001$) and DM-RA and mean deviations ($\rho = 0.45$, $P < 0.001$) were statistically significantly lower ($P = 0.02$ and $P < 0.001$, respectively) (Fig. 2).

Patients With Ocular Hypertension

The mean disc size (CSLT) in 11 eyes with macrodiscs was 2.95 ± 0.41 mm^2 (range, 2.50–3.83 mm^2) and 1.36 ± 0.17 mm^2 (range, 0.96–1.58 mm^2) in 10 microdiscs. Corresponding mean BMO areas were 2.41 ± 0.41 mm^2 (range, 1.75–3.04 mm^2) and 1.51 ± 0.34 mm^2 (range, 1.12–2.10 mm^2),

Table 4. ROC Analysis for Sensitivity Assessment of Morphometric Parameters at 95% Specificity

	Glaucoma Patients Versus Controls										
	All Patients					Macrodiscs			Microdiscs		
Parameter	Sensitivity*	95% CI†	AUC	AUC 95% CI‡	pAUC§	AUC	AUC 95% CI‡	pAUC§	AUC	AUC 95% CI‡	pAUC§
BMO-MRA	62%	0.47–0.79	0.89	0.85–0.94	0.14	0.96	0.93–0.99	0.16	0.83	0.74–0.92	0.12
BMO-MRW	54%	0.39–0.66	0.80	0.74–0.86	0.12	0.96	0.93–0.99	0.17	0.82	0.73–0.92	0.10
RNFL thickness	52%	0.22–0.66	0.84	0.78–0.89	0.11	0.88	0.81–0.95	0.12	0.79	0.70–0.89	0.11
DM-RA	47%	0.35–0.63	0.86	0.82–0.91	0.11	0.91	0.86–0.97	0.14	0.69	0.57–0.80	0.08

BMO-MRW, Bruch's membrane opening minimal rim width; CI, confidence interval; CSLT, confocal laser scanning tomography; DM-RA, Disc margin rim area; pAUC, partial area under curve; RNFL, retinal nerve fiber layer; ROC, receiver operator characteristic.

* At 95% specificity.

† Asymptotic 95% CI.

‡ Asymptotic 95% CI.

§ pAUC, partial area under the curve for specificity of 1–0.8.

respectively. Table 3 displays global morphometric parameter including sectorial data. In comparison to the 89 nonglaucomatous controls, no difference could be shown for any of the parameters. All morphometric parameters differed significantly between OHT and glaucoma patients ($P < 0.001$).

Comparative Analysis Between Diagnostic Groups

Receiver operating characteristic analyses were performed to assess and compare the diagnostic power of the morphometric parameters in this study. Because of the statistically confirmed congruence of baseline ONH parameters, OHT patients were added to the control group. For the entire group of 207 eyes, the calculated AUC results and sensitivity at 95% specificity to differentiate glaucoma patients from controls were 0.89 and 62% for BMO-MRA, 0.86 and 47% for DM-RA, 0.84 and 52% for RNFL thickness, and 0.80 and 54% for BMO-MRW (Table 4). AUC for BMO-MRA was significantly larger compared with BMO-MRW ($P < 0.001$) and with RNFL thickness ($P = 0.02$, Table 5). Regarding partial AUC (pAUC) for specificities between 0.8 and 1, pAUC of BMO-MRA was significantly larger than all three other morphometric parameters with $P < 0.001$ in comparison BMO-MRW, $P = 0.03$ compared to RNFL thickness, and $P = 0.01$ compared to DM-RA (Table 6). Cutoff points at 95% specificity were 0.78 mm^2 for BMO-MRA, 166.09 µm for BMO-MRW, 54.00 µm for RNFL, and 0.83 mm^2 for DM-RA in CSLT.

In macrodiscs, matching disc sizes in the control group showed a further increase in AUC to 0.96 for BMO-based minimum rim area measurement. In microdiscs, compared to other morphometric parameters, the BMO-MRA AUC was highest at 0.83. Separate analysis of participants with macrodiscs or with microdiscs shows a major decrease of the difference in AUC and pAUC between BMO-MRA and BMO-MRW (Table 4). Figure 3 illustrates ROC analysis for all morphometric parameters analyzed in this study.

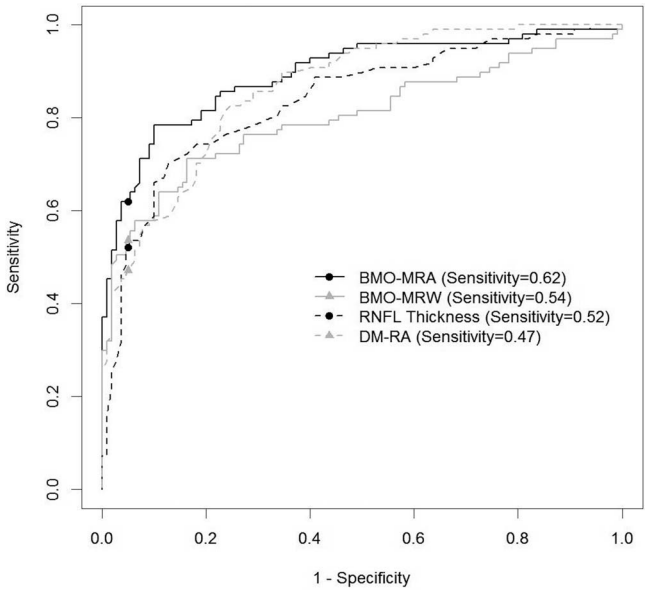

Figure 3. ROC analysis of morphometric optic disc parameters for discrimination of glaucoma patients from normal controls with sensitivities at 95% specificity.

Discussion

With increasing use of BMO-based SD-OCT in glaucoma diagnostics, the ability of different morphometric parameters to differentiate glaucomatous damage is analyzed and challenged for different ONH characteristics.[8–10] These are small or large discs, myopic discs, tilted disc, and other papillary anomalies. While Malik et al.[21] tested 130 individuals with myopic discs, we recently published reference data for 102 controls in SD-OCT analysis in nonglaucomatous large optic discs.[19,21]

Bruch's membrane opening-MRW of all the commercially available parameters, has been shown to have the highest sensitivity in discrimination of glaucoma patients from normal controls.[9] Bruch's membrane opening-based minimum rim area (BMO-MRA) analysis has been proposed as the next step in advancement of the technique.[1,12] The findings of the present study of BMO-MRA assessment in macro- and microdiscs allow

Table 5. Delong Test to Compare ROC Analysis Results of Morphometric Parameters

Parameter	AUC 1	Parameter 2	AUC 2	*P* Value
BMO-MRA	0.89	BMO-MRW	0.80	<0.001
BMO-MRA	0.89	RNFL thickness	0.84	0.017
BMO-MRA	0.89	DM-RA	0.86	0.293
BMO-MRW	0.80	RNFL thickness	0.84	0.192
BMO-MRW	0.80	DM-RA	0.86	0.071
RNFL thickness	0.84	DM-RA	0.86	0.408

AUC, area under curve; BMO-MRW, Bruch's membrane opening minimal rim width; DM-RA, disc margin rim area; RNFL, retinal nerve fiber layer; ROC, receiver operator characteristic.

Table 6. Bootstrap Estimated *P* Values For Comparing Partial AUCs Between Specificities of 0.8 and 1

Parameter	pAUC 1	Parameter 2	pAUC 2	*P* Value
BMO-MRA	0.14	BMO-MRW	0.12	<0.001
BMO-MRA	0.14	RNFL thickness	0.11	0.034
BMO-MRA	0.14	DM-RA	0.11	0.010
BMO-MRW	0.12	RNFL thickness	0.11	0.770
BMO-MRW	0.12	DM-RA	0.11	0.574
RNFL thickness	0.11	DM-RA	0.11	0.830

AUC, area under curve; BMO-MRW, Bruch's membrane opening minimal rim width; DM-RA, disc margin rim area; pAUC, partial area under the curve; RNFL, retinal nerve fiber layer; ROC, receiver operator characteristic.

the following conclusions. For a study group consisting of the full range of very large and small disc sizes, BMO-MRA offers superior diagnostic power to detect glaucoma compared to other currently used morphometric parameters. For a mixed group of micro- and macrodiscs, the SD-OCT parameters BMO-MRW and RNFL thickness do not significantly exceed the CSLT parameter DM-RA in diagnostic power. For microdiscs only, superiority of SD-OCT-based BMO-MRW and RNFL thickness measurements compared with CSLT evaluation could already be shown.[22] Therefore, for one-dimensional morphometric parameters, adapting the control group regarding disc size seems crucial to improve diagnostic power. The reasoning behind this is that normative values vary significantly with disc size.

The parameter BMO-MRA offers comparability in assessment of neuroretinal rim tissue between large differences in discs sizes. Overall sensitivities at 95% specificity and AUC results are in line with the published data of Chauhan et al.,[10] Malik et al.,[21] and the best correlation of BMO-MRA and mean deviation in visual field testing are similar to the results published by Gardiner et al.[1]

The structure-function relationship correlated at high significance levels, implying the superiority of BMO-based parameters in correlation to mean deviation in visual field testing. In other studies, the structure-function relationship varied for different examination techniques, diagnoses, and patients' characteristics.[11,28–30] Gardiner et al.[31] recently showed that peripapillary RNFL thickness may be superior compared with BMO-MRW and BMO-MRA in follow-up assessment of glaucoma patients by higher correlation to progression of visual field defects. For macro- and microdiscs, that hypothesis needs to be tested in a follow-up study.

Limitations of our study include the retrospective study set up and potential selection bias as a result of patient exclusion because of data inconsistencies or lacking image quality. The relatively large sample size in the present study reduces this possible bias. Controls were recruited from nonglaucomatous patients examined at our center, fulfilling all inclusion and no exclusion criteria of this study. In consequence, data for our patients may not be fully representative in an epidemiologic context. Availability of prospective data on normal micro- and macrodiscs is limited. Further prospective studies in normal controls also analyzing individuals with macro- and microdiscs would be helpful. Bruch's membrane opening-based minimum rim area was calculated using localized minimization of the minimum surface spanned between BMO and ILM. Hence, this approach may not accurately reflect the true total minimum area through which the nerve fibers pass. Modifications of BMO-MRA calculation using globalized optimization where one optimization is performed in all (typically 48) degrees of freedom simultaneously, need to be evaluated in future studies.

To summarize the main conclusions of the present study, BMO-MRW is significantly different between small and large discs in nonglaucomatous normal controls. Novel two-dimensional BMO-MRA equalizes disc size dependency, as it serves as an input factor to calculate the rim area. Furthermore, BMO-MRA surpasses other parameters in diagnostic power to detect glaucoma in a mixed group of small and large optic discs. Integration in the routine evaluation software could improve diagnostic performance of the technique and should be considered by the manufacturer.

Acknowledgments

The authors thank the technical experts in our imaging laboratory and those for 2240 "(Lymph-) Angiogenesis And Cellular Immunity In Inflammatory Diseases Of The Eye" for their support.

Disclosure: **P. Enders**, None; **W. Adler**, None; **F. Schaub**, None; **M.M. Hermann**, None; **T. Dietlein**, None; **C. Cursiefen**, None; **L.M. Heindl**, None

References

1. Gardiner SK, Ren R, Yang H, Fortune B, Burgoyne CF, Demirel S. A method to estimate the amount of neuroretinal rim tissue in glaucoma: comparison with current methods for measuring rim area. *Am J Ophthalmol*. 2014;157:540–549.
2. Reis AS, O'Leary N, Yang H, et al. Influence of clinically invisible, but optical coherence tomography detected, optic disc margin anatomy on neuroretinal rim evaluation. *Invest Ophthalmol Vis Sci*. 2012;53:1852–1860.
3. Reis AS, Sharpe GP, Yang H, Nicolela MT, Burgoyne CF, Chauhan BC. Optic disc margin anatomy in patients with glaucoma and normal controls with spectral domain optical coherence tomography. *Ophthalmology*. 2012;119:738–747.
4. Chen TC. Spectral domain optical coherence tomography in glaucoma: qualitative and quantitative analysis of the optic nerve head and retinal nerve fiber layer (an AOS thesis). *Trans Am Ophthalmol Soc*. 2009;107:254–281.
5. Povazay B, Hofer B, Hermann B, et al. Minimum distance mapping using three-dimensional optical coherence tomography for glaucoma diagnosis. *J Biomed Opt*. 2007;12:041204.
6. Abramoff MD, Lee K, Niemeijer M, et al. Automated segmentation of the cup and rim from spectral domain OCT of the optic nerve head. *Invest Ophthalmol Vis Sci*. 2009;50:5778–5784.
7. Mwanza JC, Oakley JD, Budenz DL, Anderson DR. Cirrus optical coherence tomography normative database study G. Ability of cirrus HD-OCT optic nerve head parameters to discriminate normal from glaucomatous eyes. *Ophthalmology*. 2011;118:241–248.
8. Chauhan BC, Burgoyne CF. From clinical examination of the optic disc to clinical assessment of the optic nerve head: a paradigm change. *Am J Ophthalmol*. 2013;156:218–227.
9. Chauhan BC, Danthurebandara VM, Sharpe GP, et al. Bruch's membrane opening minimum rim width and retinal nerve fiber layer thickness in a normal white population: a multicenter study. *Ophthalmology*. 2015;122:1786–1794.
10. Chauhan BC, O'Leary N, Almobarak FA, et al. Enhanced detection of open-angle glaucoma with an anatomically accurate optical coherence tomography-derived neuroretinal rim parameter. *Ophthalmology*. 2013;120:535–543.
11. Bowd C, Zangwill LM, Medeiros FA, et al. Structure-function relationships using confocal scanning laser ophthalmoscopy, optical coherence tomography, and scanning laser polarimetry. *Invest Ophthalmol Vis Sci*. 2006;47:2889–2895.
12. Muth DR, Hirneiss CW. Structure-function relationship between Bruch's membrane opening-based optic nerve head parameters and visual field defects in glaucoma. *Invest Ophthalmol Vis Sci*. 2015;56:3320–3328.

13. Gardiner SK, Johnson CA, Cioffi GA. Evaluation of the structure-function relationship in glaucoma. *Invest Ophthalmol Vis Sci*. 2005;46:3712–3717.
14. Anton A, Yamagishi N, Zangwill L, Sample PA, Weinreb RN. Mapping structural to functional damage in glaucoma with standard automated perimetry and confocal scanning laser ophthalmoscopy. *Am J Ophthalmol*. 1998;125:436–446.
15. Anderson RS. The psychophysics of glaucoma: improving the structure/function relationship. *Prog Retin Eye Res*. 2006;25:79–97.
16. Caprioli J. Correlation of visual function with optic nerve and nerve fiber layer structure in glaucoma. *Surv Ophthalmol*. 1989;33(suppl):319–330.
17. Garway-Heath DF, Holder GE, Fitzke FW, Hitchings RA. Relationship between electrophysiological, psychophysical and anatomical measurements in glaucoma. *Invest Ophthalmol Vis Sci*. 2002;43:2213–2220.
18. Harwerth RS, Carter-Dawson L, Smith EL III, Crawford ML. Scaling the structure-function relationship for clinical perimetry. *Acta Ophthalmol Scand*. 2005;83:448–455.
19. Enders P, Schaub F, Hermann MM, Cursiefen C, Heindl LM. Neuroretinal rim in non-glaucomatous large optic nerve heads: a comparison of confocal scanning laser tomography and spectral domain optical coherence tomography [published online ahead of print April 26, 2016]. *Br J Ophthalmol*. doi:10.1136/bjophthalmol-2015-307730.
20. Schlottmann PG, De Cilla S, Greenfield DS, Caprioli J, Garway-Heath DF. Relationship between visual field sensitivity and retinal nerve fiber layer thickness as measured by scanning laser polarimetry. *Invest Ophthalmol Vis Sci*. 2004;45:1823–1829.
21. Malik R, Belliveau AC, Sharpe GP, Shuba LM, Chauhan BC, Nicolela MT. Diagnostic Accuracy of optical coherence tomography and scanning laser tomography for identifying glaucoma in myopic eyes. *Ophthalmology*. 2016;123:1181–1189.
22. Enders P, Schaub F, Nikoluk R, Hermann MM, Heindl LM. The use of Bruch's membrane opening-based optical coherence tomography of the optic nerve head for glaucoma detection in micro-discs [published online ahead of print July 19, 2016]. *Br J Ophthalmol*. doi:10.1136/bjophthalmol-2016-308957.
23. Eurpean Glaucoma Society. *Terminology and Guidelines for Glaucoma*. 4th ed. Savona, Italy: PubliComm; 2014.
24. Aulhorn E. [Subjective examination methods in glaucoma diagnosis]. *Buch Augenarzt*. 1976;128–139.
25. Aulhorn E. [Clinical function test in glaucoma]. *Buch Augenarzt*. 1971;56:15–27.
26. Aulhorn E. [Visual field in glaucoma]. *Ophthalmologica*. 1969;158:469–487.
27. Obuchowski NA. ROC analysis. *AJR Am J Roentgenol*. 2005;184:364–372.
28. Pollet-Villard F, Chiquet C, Romanet JP, Noel C, Aptel F. Structure-function relationships with spectral-domain optical coherence tomography retinal nerve fiber layer and optic nerve head measurements. *Invest Ophthalmol Vis Sci*. 2014;55:2953–2962.
29. Nilforushan N, Nassiri N, Moghimi S, et al. Structure-function relationships between spectral-domain OCT and standard achromatic perimetry. *Invest Ophthalmol Vis Sci*. 2012;53:2740–2748.
30. Lee JR, Jeoung JW, Choi J, Choi JY, Park KH, Kim YD. Structure-function relationships in normal and glaucomatous eyes determined by time- and spectral-domain optical coherence tomography. *Invest Ophthalmol Vis Sci*. 2010;51:6424–6430.
31. Gardiner SK, Boey PY, Yang H, Fortune B, Burgoyne CF, Demirel S. Structural measurements for monitoring change in glaucoma: comparing retinal nerve fiber layer thickness with minimum rim width and area. *Invest Ophthalmol Vis Sci*. 2015;56:6886–6891.

Investigative Ophthalmology & Visual Science